

Refractive Effects in the Maritime Boundary Layer

Daniel Betteridge

Brett Nener

School of Electrical, Electronic and Computer Engineering

Stephen Hoefs

CEED Client: DSTO

Abstract

The project entitled “Refractive Effects in the Maritime Boundary Layer” focuses on understanding how refraction within 100m of the ocean’s surface affects visual range and prediction of false horizons that occur due to these effects. At the current stage of the project an analytical model of refraction has been implemented in MATLAB that provides raypaths given the variables of distance, refractive index and launch angle; The next stage involves coupling this with a simple atmospheric model to allow input of wind speed, air and sea temperature and humidity to predict under what conditions refractive effects will occur. The code will be extended to apply an estimation of refractive effects to a still image under certain conditions to give a visual example of how they will appear.

1. Introduction

This project continues from the previous work done by Brett Nener for the DSTO where he developed an analytical model of refraction that allowed for improved accuracy in calculating raypaths with very small changes (order of 10^{-6} or smaller) in the refractive index, The project is being undertaken to build on this work to provide a tool that can be used by the DSTO and their submariners to predict and analyse these refractive effects in areas of operation such as horizon and enemy detection and to allow improved operational efficiency over existing models.

1.1 Current state of the art

In terms of current methods of solving refractive raypath calculations, there are several that are used. These methods are all numerical in nature which, due to the numerous thin layers of varying refractive index that make up the atmosphere, leads to a compounding of errors as the ray travels over the large distance that is being considered in this application (tens of kilometres) and therefore a loss of accuracy over long distances.

There are a few existing studies into combining atmospheric modelling, refractive effects modelling and analysis carried out by the US and Canadian navy. They do offer good insight and utilise a simple but accurate method for predicting temperature, pressure and humidity, however they use numerical methods to produce refractive raypaths which often leads to compounding errors.

2. Development

The project utilises models of the marine boundary layer in addition to refractive index prediction models to provide a model for refractive effects in the Marine boundary layer.

The basis of this meteorological modelling is the similarity theory of Monin and Obukhov for near surface atmospheres (Forand, 1999, p11). This theory allows for boundary layer profiling utilising only the basic parameters listed above and generates six different variables that are used to describe the boundary layer in question.

$$\Delta u(z) = u(z) - u_0 = \frac{u_*}{k} \left[\ln \left(\frac{z}{z_{0u}} \right) + \Psi(z; L) - \Psi(z_{0u}; L) \right] \quad (1)$$

$$\Delta \Theta(z) = \Theta(z) - \Theta_0 = \frac{\Theta_*}{k} \left[\ln \left(\frac{z}{z_{0\Theta}} \right) + \Psi_\Theta(z; L) - \Psi_\Theta(z_{0\Theta}; L) \right] \quad (2)$$

$$\Delta q(z) = q(z) - q_0 = \frac{q_*}{k} \left[\ln \left(\frac{z}{z_{0q}} \right) + \Psi(z; L) - \Psi(z_{0q}; L) \right] \quad (3)$$

Fundamental boundary layer equations 1, 2, 3: These equations are used to estimate values for wind, virtual potential temperature and humidity with height based on the six boundary layer parameters and the Monin-Obukhov length L . (Forand, 1999, p11)

From measurements taken at the ocean surface (sea surface temperature T_s) and measurements taken at another arbitrary height within the boundary layer (Air temperature $T(z_1)$, Pressure $P(z_1)$, relative humidity $H_r(z_1)$, wind speed $u(z_1)$) we have two boundaries from which to derive solutions:

$$u_0 = u(z_{0u}) = 0 \quad (4)$$

$$q_0 = q(z_{0q}) = \frac{\mu H_r(T_s) P_w^s(T_s)}{[P_a(0) + \mu H_r(T_s) P_w^s(T_s)]} \quad (5)$$

$$\Theta_0 = \Theta(z_{0\Theta}) = T_s \left[1 + (1 - \mu) \left(\frac{q_0}{\mu} \right) \right] \left[\frac{1000}{P_0} \right]^{\frac{\gamma-1}{\gamma}} \quad (6)$$

Sea level boundary: Wind is zero, relative humidity is 98.2% according to the model used and heat is dependent on humidity, pressure and sea surface temperature. (Forand, 1999, p10)

The upper boundary equations are almost identical however T_s, q_0, P_0 are replaced by $T(z_1), q(z_1), P(z_1)$ where z_1 is the height where the measurements are made, in addition u_0 is replaced by the wind speed measurement at height z_0 where z_0 can be equal to or different from z_1 .

Our six variables of particular interest are $u_*, q_*, \Theta_*, z_{0u}, z_{0q}, z_{0\Theta}$ which define wind, humidity and heat behaviour for the boundary layer.

$$L = \frac{u_*^2 T_{vm}}{kg \Theta_*} \quad (7)$$

Monin-Obukhov length: The other important parameter in the solution of the boundary layer equations, used for normalising the height from z to z/L . (Forand, 1999, p3)

$$T_v = \left[1 + (1 - \mu) \left(\frac{q}{\mu} \right) \right] T \quad (8)$$

$$\Theta = T_v \left(\frac{1000}{P} \right)^{\frac{\gamma-1}{\gamma}} \quad (9)$$

Temperature equations: Using these equations and the above variables/equations we can determine the temperature at a particular height in the boundary layer. (Forand, 1999, p7)

The second component that will be included utilises the method developed by Fowkes and Nener (Nener, Fowkes and Borredon, 2003, p871), taking the temperature, humidity and pressure profiles generated in the first part it will generate a refractive index profile and then fit that profile to the closest matching function (Linear, Quadratic, Exponential).

Once the closest matching function is found along with its defining constants these constants are then used with the analytical solution method proposed by Nener (Nener, Fowkes and Borredon, 2003, p871) to plot the raypath over a given range for a variety of angles. Once calculated, the path description also allows calculation of other items such as magnification and shows us how the rays may have increased in elevation or been inverted while travelling through the given refractive profile.

$$n(z) = (1 + \delta n'(z')) \quad (10)$$

Refractive index profile: Formula that describes how the refractive index profile changes with height $\delta = 10^{-6}$, changes in refractive index are very small. (Nener, Fowkes and Borredon, 2003, p869)

$$n'(z') = a_2(z' - 1)^2 + a_1(z' - 1) \quad (11)$$

Describes the change of the refractive index with height, this can be linear or quadratic in this form of the equation but can be extended to higher orders and exponentials. (Nener, Fowkes and Borredon, 2003, p869)

$$z'_0 - 1 = \frac{1}{2}(kx'^2 + 2\gamma'_0 x') \quad (12)$$

Constant refractive index: z'_0 is scaled arrival height, $k = 1$ for round earth γ'_0 is scaled launch angle and x' is scaled distance. (Nener, Fowkes and Borredon, 2003, p870)

$$z' - 1 = \frac{1}{2}[(k + \eta a_1)x'^2 + 2\gamma'_0 x'] \quad (14)$$

Linear refractive profile: z' is scaled arrival height, $k=1$, $\eta = 1$ for a round earth, $a_1 \neq 0$, $a_2 = 0$ for the linear case. (Nener, Fowkes and Borredon, 2003, p871)

$$z' - 1 = \begin{cases} -\zeta + \zeta \cos(\sqrt{-2\eta a_2}) + \left[\frac{\sin(\sqrt{-2\eta a_2})}{\sqrt{-2\eta a_2}} \right] \gamma'_0 & \text{for } a_2 < 0 \\ -\zeta + \zeta \cosh(\sqrt{2\eta a_2}) + \left[\frac{\sinh(\sqrt{2\eta a_2})}{\sqrt{2\eta a_2}} \right] \gamma'_0 & \text{for } a_2 > 0 \end{cases} \quad (15)$$

Quadratic profile: the calculation of the final height depends on whether a_2 is greater or less than 0 i.e. whether the profile is concave or convex as this affects how the rays are refracted. (Nener, Fowkes and Borredon, 2003, p871)

2.1 Diagrams and Figures

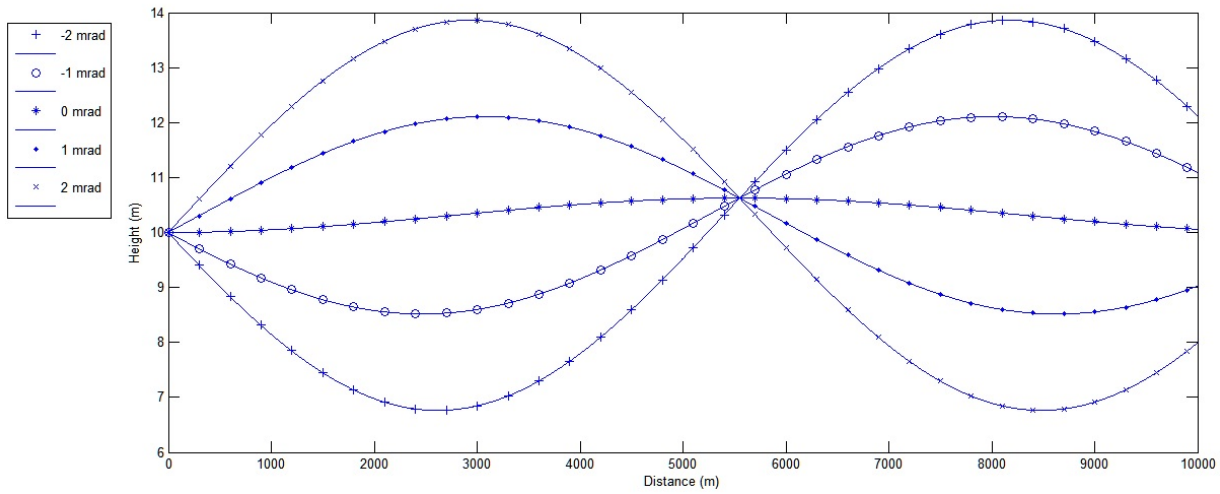


Figure 1 Path of rays launched from a height of 10 metres at angles between 2mrads and -2mrads with $a_1 = 0, a_2 = -16$ and therefore a concave quadratic profile. The above are generated by my implementation of the equation in (Nener, Fowkes and Borredon, 2003, p871)

Figure 1 is an example of a concave quadratic variation in the refractive index with height, we can see from this figure that under such conditions at large distances the image will be an inverted version of the source. Depending on the distance and the degree of change in refractive index this will determine how magnified the source appears to a distant viewer. This can be easily calculated and will play an important role in this project in allowing the modification of images to create the appearance of mirage-like effects.

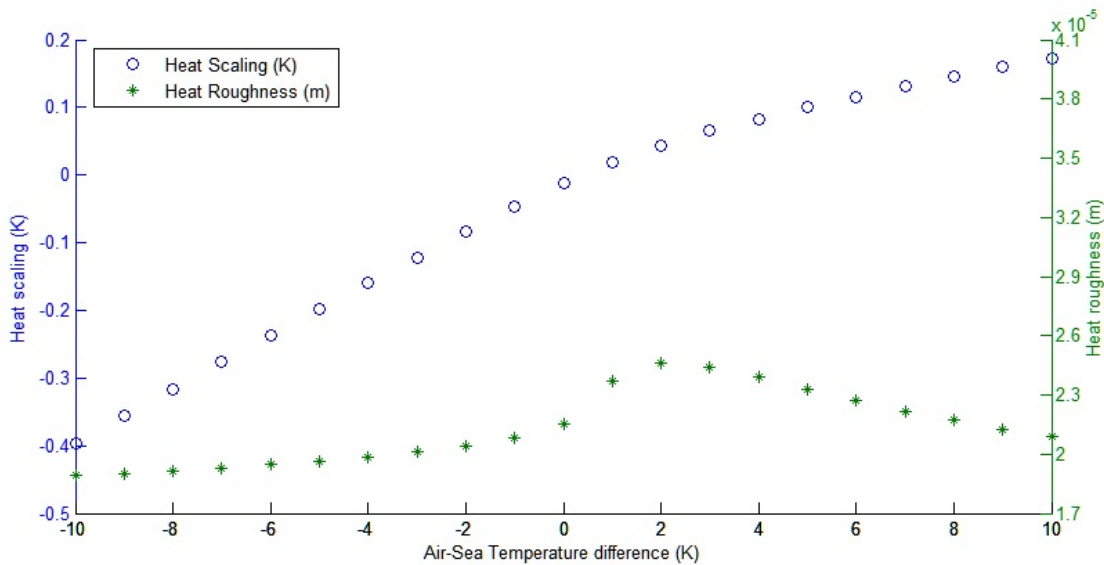


Figure 2 Virtual potential temperature scaling and roughness height for varying ASTD, $z_1 = 12m, z_0 = 22.5m, T_s = 285.65 K, P_a = 1026mbar, u_a = 5ms^{-1}$

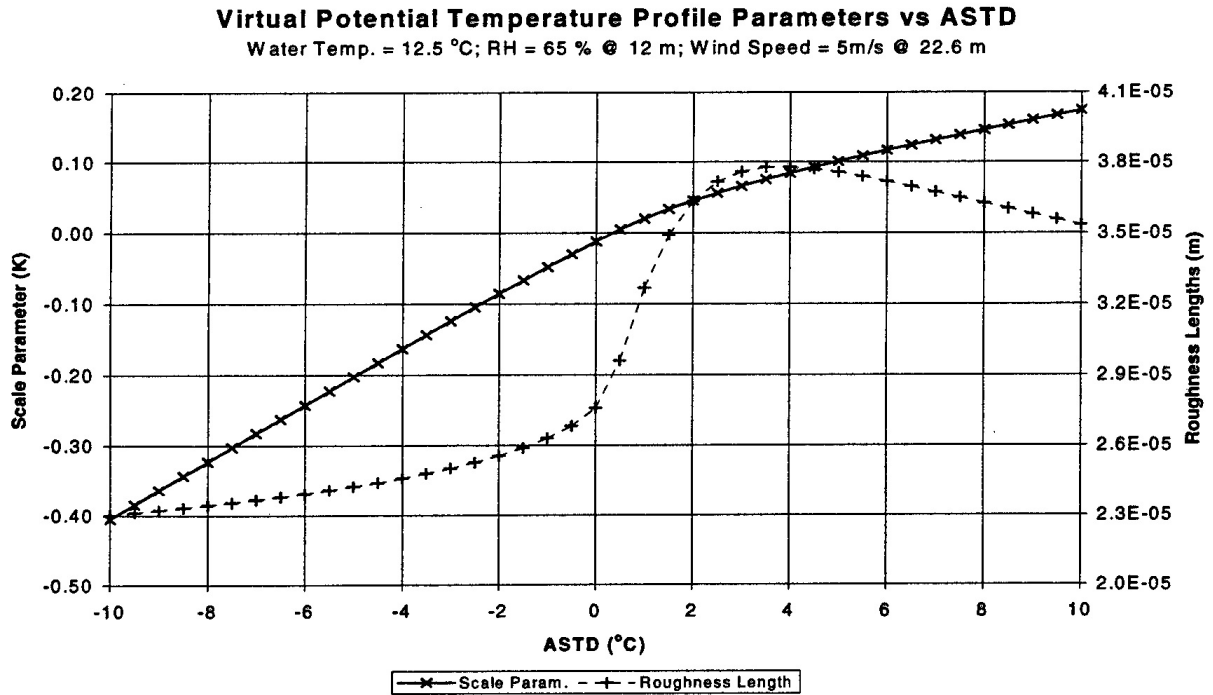


Figure 3 Virtual potential temperature scaling and roughness height for the same conditions as Figure 2, Diagram from (Forand, 1999, p60)

Figure 2 and Figure 3 display the Virtual potential temperature scaling and roughness heights. From these two graphs we can see that presently there is a very good fit for the VPT scaling variable between Figure 2 and 3 but the roughness height seems to have been compressed and shifted downwards in Figure 2 compared to Figure 3.

3. Results and Discussion

Variable	Current study	Forand
z_{0u}	4.1393×10^{-5}	2.68×10^{-5}
$z_{0\theta}$	2.4770×10^{-5}	3.837×10^{-5}
z_{0q}	2.1295×10^{-4}	3.066×10^{-4}
u_*	1.02×10^{-1}	9.81×10^{-2}
Θ_*	1.0498×10^{-1}	1.055×10^{-1}
q_*	1.7482×10^{-5}	1.756×10^{-5}
L	7.1179	6.557

Table 1 Comparison of current scaling variables and roughness heights to (Forand, 1999, p 57) for $T_s = 278.15K$, $T_a = 283.15K$, $P_a = 1010mbar$, $u_a = 5 \frac{m}{s}$, $H_r = 80\%$ and a measurement height of 15metres.

Table 1 is not consistent between the roughness heights produced by the current model and those calculated by (Forand, 1999, p57), however the values for u_* , Θ_* , q_* show a error of 4.442% for q_* compared to the values suggested by Forand and an error of only 0.492% for

Θ_* . This suggests further refinement is required in the implementation of the model to improve the iterative process that is used to refine the roughness heights and scaling values.

The process does currently produce reasonable values of temperature which fall within a few degrees kelvin of results produced by (Forand, 1999, p57), with adjustments to the model this should bring the roughness heights, scaling values and temperature values in line with those in Table 1 and (Forand, 1999, p59).

4. Conclusions and Future Work

The original task was to understand the marine boundary layer and how meteorological aspects such as temperature, humidity, pressure and wind would affect propagation of light within the marine boundary layer. While this is still a work in progress the necessary models for both modelling the atmospheric conditions and the refractive effects due to these conditions are both provided within this paper. The final steps of the project lie primarily in the development of MATLAB code to implement these models and the work of verifying the results that they provide.

Future work: could include developing an improved model of the marine boundary layer that would provide more accurate results for the atmospheric variables used in calculating the refractive index. At this time the code will not take into account variations of refractive index in the x axis but this is something that could be looked into in future with more modelling to estimate small changes at the same height over distances due to waves/localised heating/weather events.

In addition to this, the model will have code to fit either a linear, quadratic or exponential profile to the refractive index profile and these values will be fed into the raypath calculator, from there it is possible to estimate variations between real and false horizons as well magnification factors and inversions caused by the refractive profile.

5. Acknowledgements

Many thanks to both Brett Nener, Stephen Hoefs and Jeremy Leggoe, for keeping me on track and making sure I knew what was expected of me throughout the entirety of the project so far.

6. References

Forand, J.L.F, 1999. THE L(W)WKD MARINE BOUNDARY LAYER MODEL. [Online]. V7.09, 5-17. Available at: <http://cradpdf.drdc-rddc.gc.ca/PDFS/zbc76/p511546.pdf> [Accessed 11 August 2014].

Nener, B.D.N; Fowkes, N.F; Borredon, L.B, 2003. Analytical models of optical refraction in the troposphere. [Online]. Vol 20, No. 5, p867-875. Available at: <http://www.opticsinfobase.org/josaa/abstract.cfm?uri=josaa-20-5-867> [Accessed 1 March 2014].